Using GPS positioning to recover a comprehensive road appearance mosaic

Ivan Sikirić
Mireo d.d.
Buzinski prilaz 32, 10000 Zagreb
e-mail: ivan.sikiric@mireo.hr

Ante Majić, Siniša Šegvić
Faculty of Electrical Engineering and Computing
Unska 3, 10000 Zagreb
e-mail: name.surname@fer.hr

***Abstract*—We describe a system that employs a GPS device and a single calibrated camera mounted on a moving vehicle to produce a road appearance map as a comprehensive mosaic of individual orthogonal views. The system first transforms the current image of the road acquired from a driver's perspective into the orthogonal view by inverse perspective mapping. The orthogonal image is aligned with previously recovered parts of the mosaic with respect to the interpolated GPS coordinates and bearing. Experiments have been performed on videos taken along public roads through Croatian countryside and small cities. The obtained results are provided and discussed.**

I. Introduction

We consider a setup in which video is captured using a GPS device and a camera mounted on a moving vehicle. The vehicle is driving down the road for which we try to obtain a comprehensive surface appearance map. We apply inverse perspective mapping [1], [2] to each of the captured video frames in order to obtain orthogonal (bird's eye) view of the road surface [3]. The GPS device provides us with the coordinates, velocity and the bearing of the vehicle once a second. In other words, we have globally consistent positional estimate for one in every 25 frames of the video. For other frames we derive the required data by interpolation. By fusing suitably aligned orthogonal views we obtain a road appearance mosaic which corresponds to the desired comprehensive map of the road surface. A surface appearance map of the road can be useful in a variety of applications. For instance, it can be used to verify appropriate placement of road surface markings, which is critical for traffic safety, especially at the crossings. It can also be used to verify the extent of road maintenance (the surface under new asphalt). Assessing the state of road surface in many countries is still performed manually by human operators, and is a time consuming and cumbersome process [4]. Providing a georeferenced road appearance mosaic would speed up and simplify this process considerably, by enabling the verification of the road markings without the need for on-location measuring. Furthermore, the recovered road surface map can be vectorized and stored in a suitable GIS database [5]. This database could be used to verify the existing cadastre maps against the actual conditions.

II. Related work

Existing approaches for obtaining road appearance mosaics and similiar forms of road appearance maps differ in the number and types of sensors installed on the acquisition vehicle and in the level of supervision required.

Given that the appearance, structure and other properties of the road are well constrained, it is possible to use a wide array of sensors which add additional cues about the road and hence improve the end result. Commonly employed sensors include stereo cameras, laser scanners, GPS, odometers, etc. Different combinations of sensors require different approaches and algorithms.

Wang et al [6] describe a system which works with data obtained by a mobile mapping vehicle equipped with an inertial navigation system, dual frequency GPS, 6-12 color cameras and an odometer. Given the GPS information, multi-camera panoramic images and sensor calibration parameters, their algorithm outputs a GIS-database-compatible road geometry information, which consists of a 3D lane line model of all the lane lines observed in the video. For each line, line type and color attributes are also available. To obtain the model they first perform a variant of inverse perspective mapping, which enables them to get an orthogonal view of the road. Orthogonal view of the road is beneficial because it simplifies detection of road surface markings. Inverse perspective mapping relies on the assumption that the road is locally planar, which is not always the case. Hence, pitch correction of the mapping is achieved by modeling the road surface profile using geolocation information. For each frame, the position of the measurement rack in a geographical coordinate system is estimated using sensor data. Using this information, it is possible to estimate the spatial trajectory of the vehicle, which corresponds to the longitudinal road surface profile. Having obtained the orthogonal image, line segments are extracted, linked, classified and added to the model.

Shi et al [7] rely on videos acquired from a vehicle equipped with an odometer, two GPS receivers, two sets of stereo camera systems and three laser scanners. By using laser scanners they obtain range data for road and roadside objects in the form of 3D point clouds. The laser data is then fused with the image data to obtain fully automated spatial positioning of road parts, which results in a road appearance map. Other interesting results with laser scanners are available in [8], [9].

There are approaches that rely on some amount of human interaction. For example, Barinova et al [10] present an algorithm for road mapping which is continuously trained to detect a road with the help of a human operator. The algorithm includes an offline learning stage and an online operation / correction stage.

There are approaches which rely on a single sensor [11], [12]. Bigorgne and Tarel [11] focus on the development of the system for continuous measurement of the geometrical visibility range on inter-urban roads. They propose a solution based on a segmentation of the road using local color features and on parametrized fitting of the segmented regions using a priori knowledge about roads. The proposed approach works well with straight roads, but authors suggest using stereo vision for curved roads. The approach does not require any interaction with the user.

To summarize, using multiple different sensors yields better maps. However, the overall cost and complexity of obtaining a map increases with the number of sensors. Depending on the application, the systems for road mapping can be fully automated or interactive. The system we would like to build is similar in spirit to the approach of Wang et al [6], as it also produces a road appearance mosaic, however we would like to achieve that using as little sensorial input as possible.

III. Assumptions and datasets

In the presented system the comprehensive mosaic is obtained by combining the following techniques: (i) inverse perspective mapping, (ii) interpolating GPS estimates. Each frame of the video is first transformed into the corresponding orthogonal view. Subsequently, the road surface mosaic is incrementally updated by aligning each orthogonal image I_i with the previous state of the mosaic recovered from the predecessors of I_i. The alignment is achieved by employing interpolated GPS estimates.

The system we propose has been evaluated on a subset of a large collection of videos obtained from a vehicle driving the countryside, suburbs and small cities in Croatia [4]. The vehicle is equipped with a single top-mounted camera, and a GPS sensor (cf. Figure 1). Hence, all obtained videos are georeferenced. Additionaly, all sensor inputs are synchronized with respect to the common clock. The employed GPS device was FV-M8 from San Jose Navigation. It has a configurable update rate of 1-5 Hz, and 3.3 m accuracy.

For simplicity, we assume local planarity of the road surface. This assumption is often violated, because the cross-section of the road is often considerably concave or sloped, to facilitate water drainage during rain. However, this assumption enables us to produce useful results without additional expensive instruments. Additionally, we assume the road plane to be constant throughout the video sequence. To be more precise, we assume that the normal of the road plane with respect to the camera, and its distance from the camera is constant. This assumption eliminates the need for road surface detection algorithms, but is unfortunately often violated as well.

Fig. 1. The vehicle used for acquisition of road videos, equipped with a single camera, a GPS receiver and an odometer. The videos are georeferenced using an on-board computer equipped with a geoinformation system.

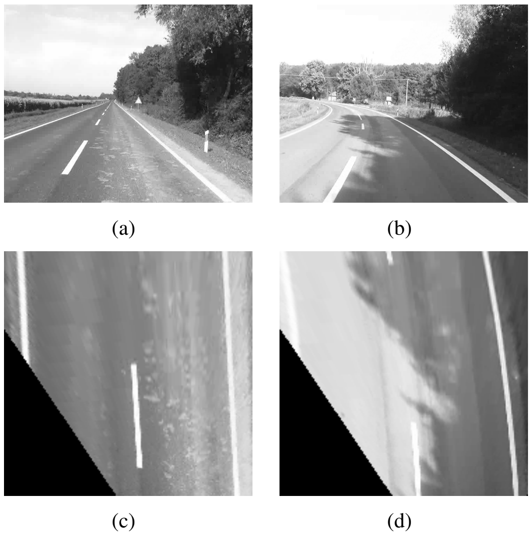

Fig. 2. Images captured from a moving vehicle (a,b) and the corresponding inverse perspective mappings (c,d). Different configurations of the road are shown: a straight road (a) is transformed into the orthogonal image (c), a slightly curved road (b) is transformed into the orthogonal image (d).

Vertical orientation of the camera (the tilt angle) can vary due to vehicle dynamics. Slight errors in orientation produce large errors in the appearance of the parts of the road that are far from the camera. Fortunately, there is little pixel data for those parts of the road, so they must be ignored in any case. Inverse mapping of the appearance of the road parts close to the camera is in many cases good enough to produce useful results, although errors are noticeable. These errors could be reduced by elevating the camera and increasing its downwards angle.

We chose to ignore the radial distortion of the camera. Radial distortion correction involves calibration of the camera that recorded the video. Different cameras were used to record the videos, and the calibration would take considerable time. Also, we wanted to examine the results obtained by simply ignoring the radial distortion.

IV. Inverse perspective mapping

A single captured video frame represents a projection of a 3D scene onto the image plane (cf. Figure 2(a) and 2(b)). This process is generally impossible to invert since it is not injective. However, we are only interested in obtaining the image of the road surface from an orthogonal perspective (cf. Figure 2(c), 2(d)), and do not need to attempt a full 3D reconstruction of the scene. If we assume that the road surface is contained in a plane, and that it is not occluded by other objects, then we can employ inverse perspective mapping [1], [2], [13] to obtain orthogonal images.

In the following, we denote the points of the plane $\mathbf{q} \in \pi$ by homogeneous coordinates [14] such that $\mathbf{q}_i = [x_i, y_i, 1]^\top \; \forall i$, where (x_i, y_i) denote the usual Cartesian coordinates in the Euclidean plane. Denote the points on the road plane as $\mathbf{q}_\mathrm{R}$, their projections to vehicle's camera plane as $\mathbf{q}_\mathrm{P}$ and their projections to the orthogonal plane as $\mathbf{q}_\mathrm{I}$. Then these points can be related by the following bijective mapping [14], [15]:

$$\mathbf{q}_{\mathrm{P}i} = \mathbf{H}_{\mathrm{RP}} \cdot \mathbf{q}_{\mathrm{R}i}, \ \forall i \tag{1}$$

$$\mathbf{q}_{\mathrm{I}i} = \mathbf{H}_{\mathrm{RI}} \cdot \mathbf{q}_{\mathrm{R}i}, \ \forall i \ . \tag{2}$$

The transformations $\mathbf{H}_{\mathrm{RP}}$ and $\mathbf{H}_{\mathrm{RP}}$ are planar projective mappings, which are often also referred to as homographies. From (1) and (2) follows:

$$\mathbf{q}_{\mathrm{I}i} = \mathbf{H}_{\mathrm{IPM}} \cdot \mathbf{q}_{\mathrm{P}i}, \ \forall i \tag{3}$$

$$\mathbf{H}_{\mathrm{IPM}} = \mathbf{H}_{\mathrm{RI}} \cdot \mathbf{H}_{\mathrm{RP}}^{-1} \ . \tag{4}$$

The homography $\mathbf{H}_{\mathrm{IPM}}$ is often referred to as inverse perspective mapping [1], [2], [13].

Once the matrix $\mathbf{H}_{\mathrm{IPM}}$ is known, the orthogonal view $\mathbf{I}_{\mathrm{orth}}$ is easily recovered from a given perspective image $\mathbf{I}_{\mathrm{persp}}$ as follows:

$$\mathbf{I}_{\mathrm{orth}}(\mathbf{q}) = \mathbf{I}_{\mathrm{persp}}(\mathbf{H}_{\mathrm{IPM}}^{-1} \cdot \mathrm{q}), \ \forall \mathbf{q} \in \mathbf{I}_{\mathrm{orth}} \ . \tag{5}$$

There are many ways for recovering the matrix $\mathbf{H}_{\mathrm{IPM}}$. The simplest one is to manually locate four known points in the perspective image, and to recover the unique mapping as the solution of a homogeneous linear system [14]. We have established an involved but somewhat more practical method whereby it suffices to select the edges of a straight road ahead, which is similar in spirit to what has been proposed in [16]. However, the following two assumptions need to hold: (i) that the internal camera parameters are known [17], and (ii) that the roll of the camera with respect to the road plane is negligible. The matrix $\mathbf{H}_{\mathrm{IPM}}$ can be calibrated beforehand (this is our current practice) [18], or continuously adapted to the dynamics of the vehicle motion by a suitable optimization procedure [16], [19].

The matrix $\mathbf{H}_{\mathrm{IPM}}$ could also be recovered by determining the appropriate motion between the physical camera and the virtual camera corresponding to the orthogonal view, using the following equation [15].

$$\mathbf{H}_{\mathrm{IPM}} = \mathbf{K}_{\mathrm{C}} \cdot (\mathbf{R} + \frac{\mathbf{T}\mathbf{n}^T}{d}) \cdot \mathbf{K}_{\mathrm{C}}^{-1} \ . \tag{6}$$

In the above equation, $\mathbf{K}_{\mathrm{C}}$ denotes intrinsic camera parameters [17], $\mathbf{R}$ and $\mathbf{T}$ rotation and translation from the physical to the virtual camera, respectively, while $\mathbf{n}$ and d denote the normal of the plane and its distance in the coordinates of the physical camera.

V. Interpolating GPS data

The GPS device provides us once a second with the global coordinates of the vehicle, the vehicle's bearing and its velocity. For any two successive measurements, we need to interpolate the data for the rest of the 24 frames of video in between. We use the approach [20], illustrated in figures 3, 4 and 5. The two successive measurements are shown in Figure 3. For the moment t we know the position of the vehicle $Q_E^A(x_E^A, y_E^A)$, its velocity v_E^A, and orientation θ_E^A. For the moment $(t+1)$, we know the position of the vehicle $Q_E^B(x_E^B, y_E^B)$, its velocity v_E^B, and orientation θ_E^B. We want to derive the positions and orientation of the vehicle in moments $t_k = (t + 0.04 \cdot k), \ k = 1, ..., 24$. To simplify the calculations, we translate and rotate the scene so as to position the vehicle in the origin, and to make the

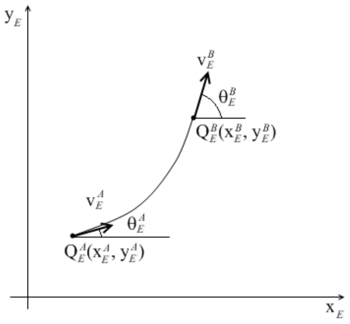

Fig. 3. GPS data in the coordinate system of Earth

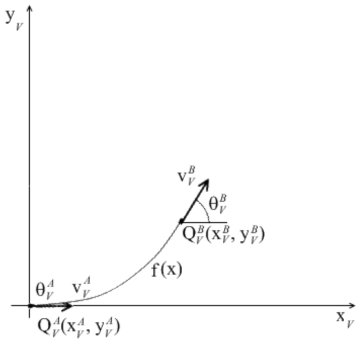

Fig. 4. GPS data in the coordinate system of the vehicle

initial orientation equal to zero. The transformed data is shown in Figure 4. We approximate the vehicle trajectory by a third degree polynomial:

$$f(x) = Ax^3 + Bx^2 + Cx + D \tag{7}$$

By observing that $f(x) = y$, $f'(x) = \tan\theta$ and $Q_V^A = 0$, we derive $C = D = 0$. We obtain A and B by solving the equations:

$$y_V^B = A(x_V^B)^3 + B(x_V^B)^2 \tag{8}$$

$$\tan\theta_V^B = 3A(x_V^B)^2 + 2Bx_V^B \tag{9}$$

We assume linear change in vehicle velocity between two endpoints, so for any time instant t_k we can determine the length of the path the vehicle travelled fom initial position in time instant t. By using discretization of $f(x)$, we avoid performing integration and approximate the interpolated vehicle positions and orientations. We finally perform the inverse rotation and translation on these positions and orientations. The result is shown in the Figure 5.

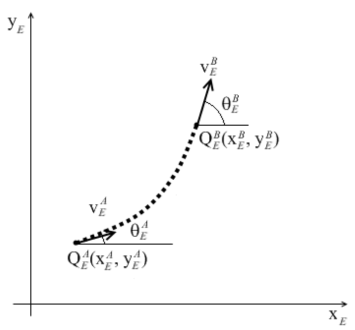

Fig. 5. Interpolated GPS data in the coordinate system of Earth

VI. ALIGNMENT OF ORTHOGONAL IMAGES USING GPS DATA

In this phase, we perform batch alignment of a series of orthogonal road images $I_1, I_2, ..., I_n$. Since we assume the road is locally planar, parts of the road appearing in two subsequent orthogonal images can be related by a transformation with 4 degrees of freedom: translation along the line of movement (i.e. direction of road), slight translation orthogonally to the line of movement, rotation along a vertical axis, and scaling (which approximates the effects of vehicle tilting). Before we can use GPS absolute position and orientation parameters (given in the spherical coordination system of Earth), we need to transform them into pixel coordinate system of the image. All vehicle positions are from a set (λ_i, φ_i), where λ_i and φ_i denote longitude and lattitude of the vehicle for image I_i. Let $[\lambda_{\min}, \lambda_{\max}]$ and $[\varphi_{\min}, \varphi_{\max}]$ respectively represent the longitude and lattitude intervals of the given set of vehicle positions. We calculate the sphere distance $d_x = d((\lambda_{\min}, \varphi_{\min}), (\lambda_{\max}, \varphi_{\min}))$ and $d_y = d((\lambda_{\min}, \varphi_{\min}), (\lambda_{\min}, \varphi_{\max}))$, where $d(P_1, P_2)$ represents the sphere distance between points P_1 and P_2. We then approximate all the vehicle positions to be locally planar and transform them to a single plane:

$$x_i = \frac{\lambda_i - \lambda_{\min}}{\lambda_{\max} - \lambda_{\min}} \cdot d_x$$

$$y_i = \frac{\varphi_i - \varphi_{\min}}{\varphi_{\max} - \varphi_{\min}} \cdot d_y$$

In order to place the orthogonal image in this plane, we need to know the following parameters: (i) distance of the camera from the road (from the image), (ii) distance of the line of the left edge of the image from the camera and (iii) number of pixels per meter. We denote these parameters by u_{C}, v_{C} and μ_{C}, respectively. Camera distance parameters u_{C} and v_{C} are illustrated in Figure 6. Parameter μ_{C} is simply a scaling factor used to transform distance in meters to distance in pixels. Fortunately, they can all be calibrated beforehand. Coordinates of the pixels of the orthogonal image i $(x^{\mathrm{ort}}_{i,j}, y^{\mathrm{ort}}_{i,j})$ range from $(0,0)$ to $(\mathrm{width}_i, \mathrm{height}_i)$ (direction of the road is roughly in the direction of the positive x-axis). Transformed coordinates are obtained as follows:

$$[x_{i,j}, y_{i,j}]^T = \mathbf{T}_{\mathrm{GPS}}[x^{\mathrm{ort}}_{i,j}, y^{\mathrm{ort}}_{i,j}]^T = \mathbf{T_2 R T_1}[x^{\mathrm{ort}}_{i,j}, y^{\mathrm{ort}}_{i,j}]^T$$

where $\mathbf{T_1}$ represents translation matrix that translates the original image by $(u_{\mathrm{C}} \cdot \mu_{\mathrm{C}}, v_{\mathrm{C}} \cdot \mu_{\mathrm{C}})$, $\mathbf{R}$ denotes rotation of the image by the angle obtained from interpolated GPS data and $\mathbf{T_2}$ denotes the rotation by $(x_i \cdot \mu_{\mathrm{C}}, y_i \cdot \mu_{\mathrm{C}})$.This

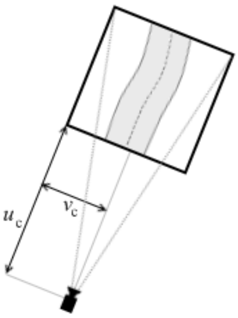

Fig. 6. Camera distance parameters

process can be used to place all of the orthogonal images into the comprehensive mosaic (cf. Figure 7).

The obtained transformation matrix $\mathbf{T}_{\mathrm{GPS}}$ is used to generate the comprehensive road mosaics in the following way:

1) Start with an empty road mosaic, and set the current video frame index to zero.
2) Obtain the orthogonal image for the current video frame.
3) Obtain the transformation matrix $\mathbf{T}_{\mathrm{GPS}}$ using interpolated GPS data.
4) Use the transformation to combine the image with the existing road mosaic. In area of image overlapping, overwrite the previous pixel values with the new ones.
5) Increment the current frame index.
6) If the current frame index is not past the last frame of the video, repeat from step 2.

Older pixel values are overwritten with the new ones because the quality of the pixel data of the common road part in subsequent images is not the same. If the vehicle is moving forward, then the corresponding part of the road has moved closer to the camera, and has better resolution in newer frames.

VII. EXPERIMENTAL RESULTS

Examples of results are shown in Figure 8. Figure 9 shows that the produced road surface mosaic is quite consistent with the corresponding satellite image, while offering substantially more details and being much cheaper to obtain. Imperfections of this approach are visible best in close-ups of road appearance, as shown in Figure 10. Some deviations and small miss-alignments can be noticed. Deviations are a result of imperfect GPS-data interpolation, and occasional miss-alignments are a consequence of relatively low accuracy of GPS data

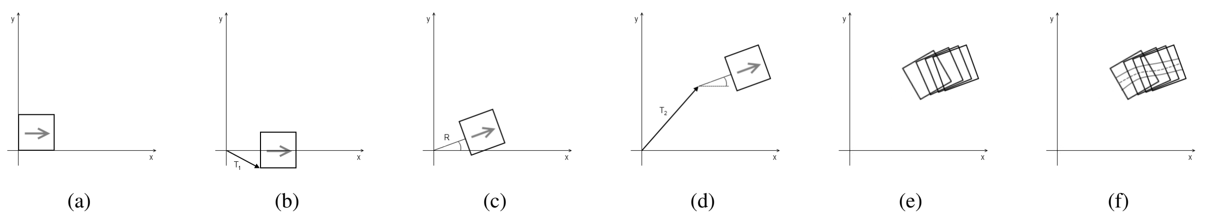

Fig. 7. Illustration of the image alignment process. Initial location of the image (a). Location of the image after translation T_1 (b). Location of the image after rotation R (c). Final location of the image, after translation T_2 (d). Location of several consecutive aligned images (e) and (f).

Fig. 8. Example segments of road appearance mosaic

(measured in meters). Notice that the left lane of the road is considerably more distorted than the right lane. This is a result of our assumption of a constant road plane.

VIII. Conclusion

The paper describes a technique for producing comprehensive road surface appearance mosaics by processing video acquired from the driver's perspective. The proposed technique does not require expensive equipment such as laser scanners. In comparison with aerial and satellite imagery the obtained road mosaics are far better in terms of image resolution and much cheaper to obtain.

The achieved results appear good enough for several useful applications in the domains of road inspection and road maintenance. For instance, the magnified mosaic in Figure 10 allows for easy assessment of the lane configuration, as well as for inspecting the shape of the cross-hatched clear zone. Additionally, in mosaics such as the one showed in Figure 10 one could easily assess the costs of recent road maintenance by detecting the areas under new asphalt.

IX. Future work

We plan to use the image-based approach to fine-tune the parameters of the transformation obtained by GPS data. We have also developed a working visual odometry subsystem which will be integrated with the road mapping framework, which might further improve the quality of the results. It might even enable us to generate the road appearance mosaic in the areas where GPS data is not available or is of low quality. We have promising results with using steerable filters to obtain road lane lines. The road lane lines can be used to additionally improve fine tuning of the transformation parameters. If any lane

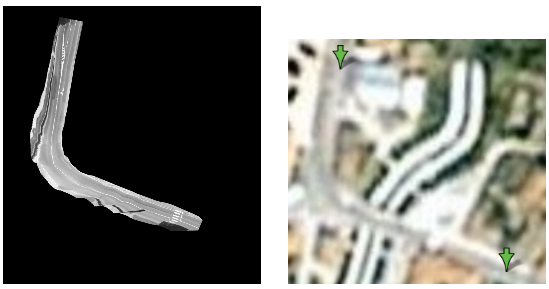

(a) (b)

Fig. 9. Comparison with ground-truth data. Road mosaic obtained by our system (a), actual appearance of the road in question (b), obtained via Google Maps (Copyright 2010 Google, 2010 DigitalGlobe, GeoEye)

line is present, we can calculate the rotation parameter. Dashed lane line can be used to impose constraints on translation parameters. Road detection simplifies removal of non-road pixels, which would improve the appearance of the results. Road plane detection could alleviate some distortions caused by constant road plane assumption. More advanced modelling of vehicle movement would be very useful. It would be used to detect possible errors in GPS data (and, later, visual odometry data).

X. Acknowledgements

This research has been jointly funded by the Croatian National Foundation for Science, Higher Education and Technological Development, and the Institute of Traffic and Communications under programme Partnership in Basic research, project number #04/20. The project web page is at http://www.zemris.fer.hr/ ssegvic/mastif

References

[1] A. Guiducci, "3d road reconstruction from a single view," *Computer Vision and Image Understanding*, vol. 70, no. 2, pp. 212–226, 1998.

[2] J. McCall and M. Trivedi, "Video-based lane estimation and tracking for driver assistance: survey, system, and evaluation," *IEEE Transactions on Intelligent Transportation Systems*, vol. 7, pp. 20–37, Mar. 2006.

[3] N. Simond, "Reconstruction of the road plane with an embedded stereo-rig in urban environments," in *Proceedings of the IEEE Intelligent Vehicles Symposium*, (Tokyo, Japan), pp. 70–75, June 2006.

[4] S. Šegvić, K. Brkić, Z. Kalafatić, V. Stanisavljević, D. Budimir, and I. Dadić, "Towards automatic assessment and mapping of traffic infrastructure by adding vision capabilities to a geoinformation inventory," in *Proceedings of MIPRO'09*, pp. 276–281, May 2009.

[5] Y. Wang, L. Bai, and M. Fairhurst, "Robust road modeling and tracking using condensation," *IEEE Transactions on Intelligent Transportation Systems*, vol. 9, pp. 570–579, Dec. 2008.

[6] C. Wang, T. Hassan, N. El Sheimy, and M. Lavigne, "Automatic road vector extraction for mobile mapping systems," in *Proc. of ISPRS*, 2008.

[7] Y. Shi, R. Shibasaki, and Z. Shi, "Towards automatic road mapping by fusing vehicle-borne multi-sensor data," in *Proc. of ISPRS*, 2008.

[8] J. K. G. Hunter, C. Cox, "Development of a commercial laser scanning mobile mapping system - streetmapper," in *Proceedings of 2nd International Workshop of the future of Remote Sensing*, 2006.

[9] J. Talaya, E. Bosch, R. Alamus, E. Bosch, A. Serra, and A. Baron, "Geomobil: the mobile mapping system from the icc," in *Proceedings of 4th International Symposium on Mobile Mapping Technology*, 2004.

[10] O. Barinova, R. Shapovalov, S. Sudakov, A. Velizhev, and A. Konushin, "Efficient road mapping via interactive image segmentation," in *Proc. of CMRT*, 2009.

[11] E. Bigorgne and J.-P. Tarel, "Backward segmentation and region fitting for geometrical visibility range estimation," in *Proc. of ACCV (2)*, pp. 817–826, 2007.

[12] F. Paetzold and U. Franke, "Road recognition in urban environment," *Image and Vision Computing*, vol. 18, pp. 377–387, 2000.

[13] S. Tan, J. Dale, A. Anderson, and A. Johnston, "Inverse perspective mapping and optic flow: A calibration method and a quantitative analysis," *Image and Vision Computing*, vol. 24, no. 2, pp. 153 – 165, 2006.

[14] R. I. Hartley and A. Zisserman, *Multiple View Geometry in Computer Vision*. Cambridge University Press, 2004.

[15] Y. Ma, S. Soatto, J. Košecká, and S. Sastry, *An Invitation to 3-D Vision: From Images to Geometric Models*. New York, USA: Springer-Verlag, 2004.

[16] M. Nieto, L. Salgado, F. Jaureguizar, and J. Cabrera, "Stabilization of inverse perspective mapping images based on robust vanishing point estimation," in *Proceedings of the IEEE Intelligent Vehicles Symposium*, (Istanbul,Turkey), pp. 315–320, June 2007.

[17] Z. Zhang, "A flexible new technique for camera calibration," *IEEE Transactions on Pattern recognition and Machine Intelligence*, vol. 22, pp. 1330–1334, Nov. 2000.

[18] A. Guiducci, "Camera calibration for road applications," *Computer Vision and Image Understanding*, vol. 79, no. 2, pp. 250–266, 2000.

[19] A. Catala Prat, J. Rataj, and R. Reulke, "Self-calibration system for the orientation of a vehicle camera," in *Proceedings of the ISPRS Commission V Symposium Image Engineering and Vision Metrology*, (Dresden, Germany), pp. 68–73, Sept. 2006.

[20] A. Majić, "Creating the map of road surface markings from georeferenced video," Master's thesis, Faculty of Electrical Engineering and Computing, Zagreb, Croatia, 2010.

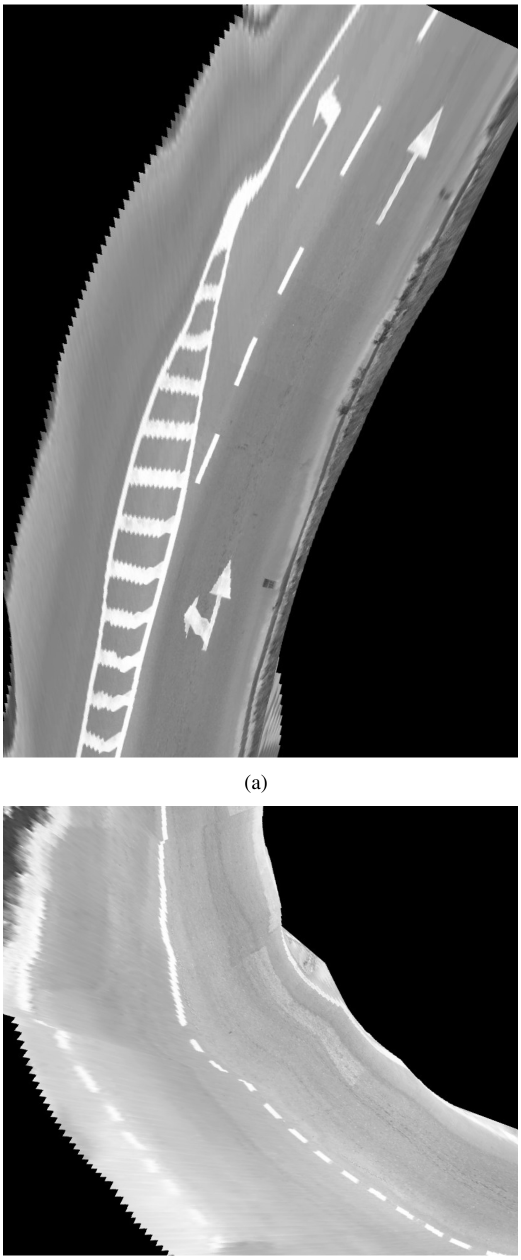

(a)

(b)

Fig. 10. Close-up on the mosaic details. Successful alignment, but great distortions on the left road lane (a) and poor alignment due to road curvature (b)